ISCI, Volume *22*

Supplemental Information

Food-Derived Compounds Apigenin and Luteolin Modulate mRNA Splicing of Introns with Weak Splice Sites

Masashi Kurata, Naoko Fujiwara, Ken-ichi Fujita, Yasutaka Yamanaka, Shigeto Seno, Hisato Kobayashi, Yusaku Miyamae, Nobuyuki Takahashi, Yasuyuki Shibuya, and Seiji Masuda

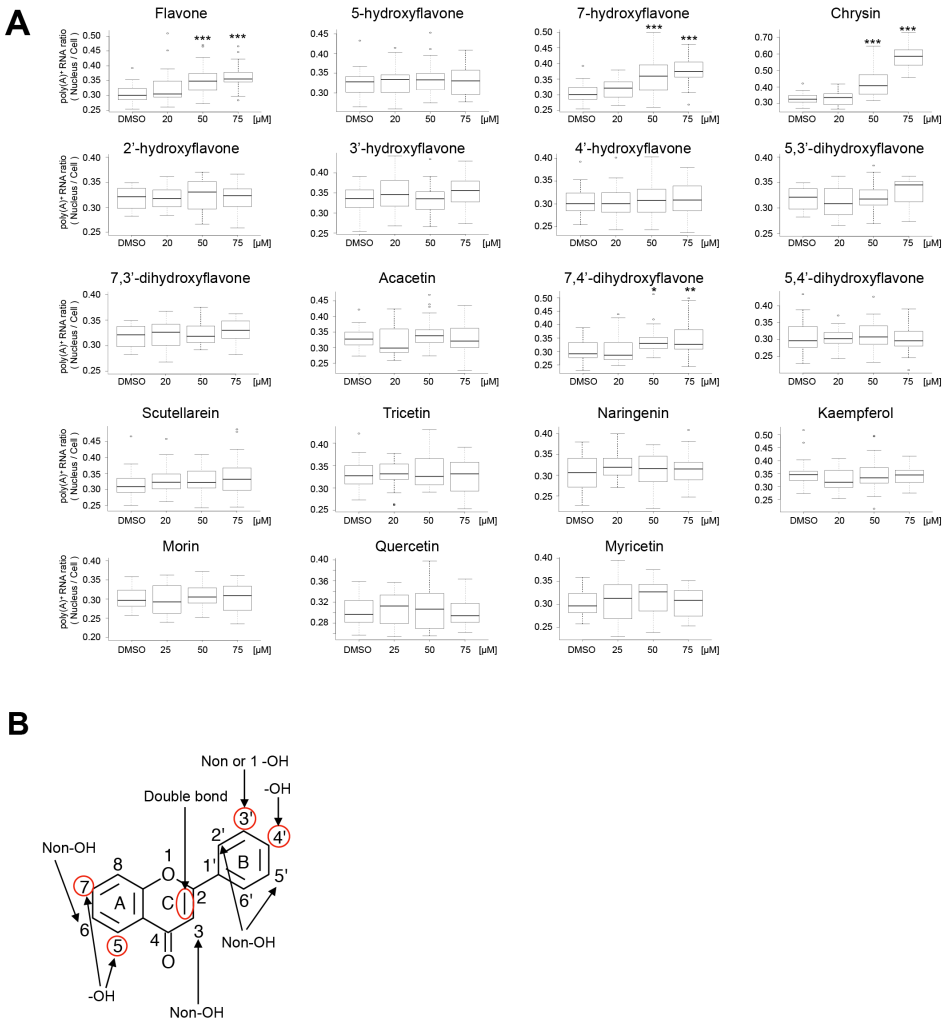

Figure S1. Accumulation of poly(A)$^+$ RNA by the indicated chemical compounds with a flavone skeleton. (Related to Figure 1)

(A) mRNA processing inhibitory activity of chemical compounds with a flavone skeleton. The ratio of nuclear distribution of mRNA is shown. The signal intensities of bulk poly(A)$^+$ RNA in the whole-cell and in the nucleus were quantified using ImageJ (n = 35). Boxes show median (center line) and upper and lower quartiles. Whiskers show the lowest and highest values. Statistical analysis was performed using one-way ANOVA followed by Dunnett's test. *p < 0.05, **p < 0.01, ***p < 0.001.

(B) Chemical structure with strong mRNA processing inhibitory activity.

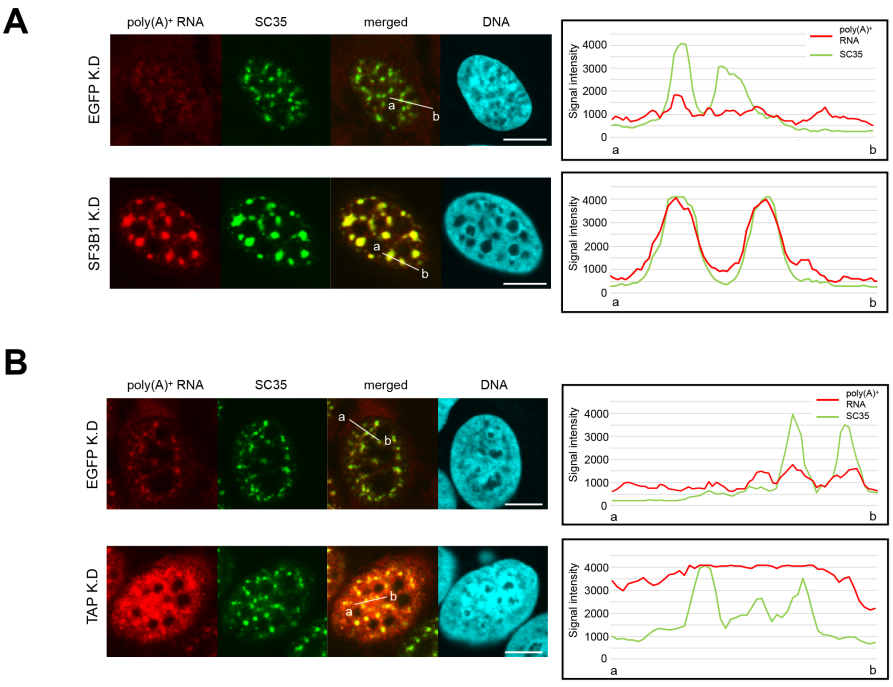

Figure S2. Localization of poly(A)$^+$ RNA in cells depleted of splicing factor, SF3B1, and mRNA exporter, TAP. (Related to Figures 2 and 3)

(A) and (B) Localization of poly(A)$^+$ RNA in U2OS cells. Poly(A)$^+$ RNA localization (red) was observed in SF3B1 (A) and TAP (B) knockdown conditions. SC35 (green) was used to stain the nuclear speckle. DAPI (blue) was used to visualize the nuclei. Scale bar, 10 μm. In right panels, signal intensities of poly(A)$^+$ RNA and SC35 were plotted between a and b lines in the left panels.

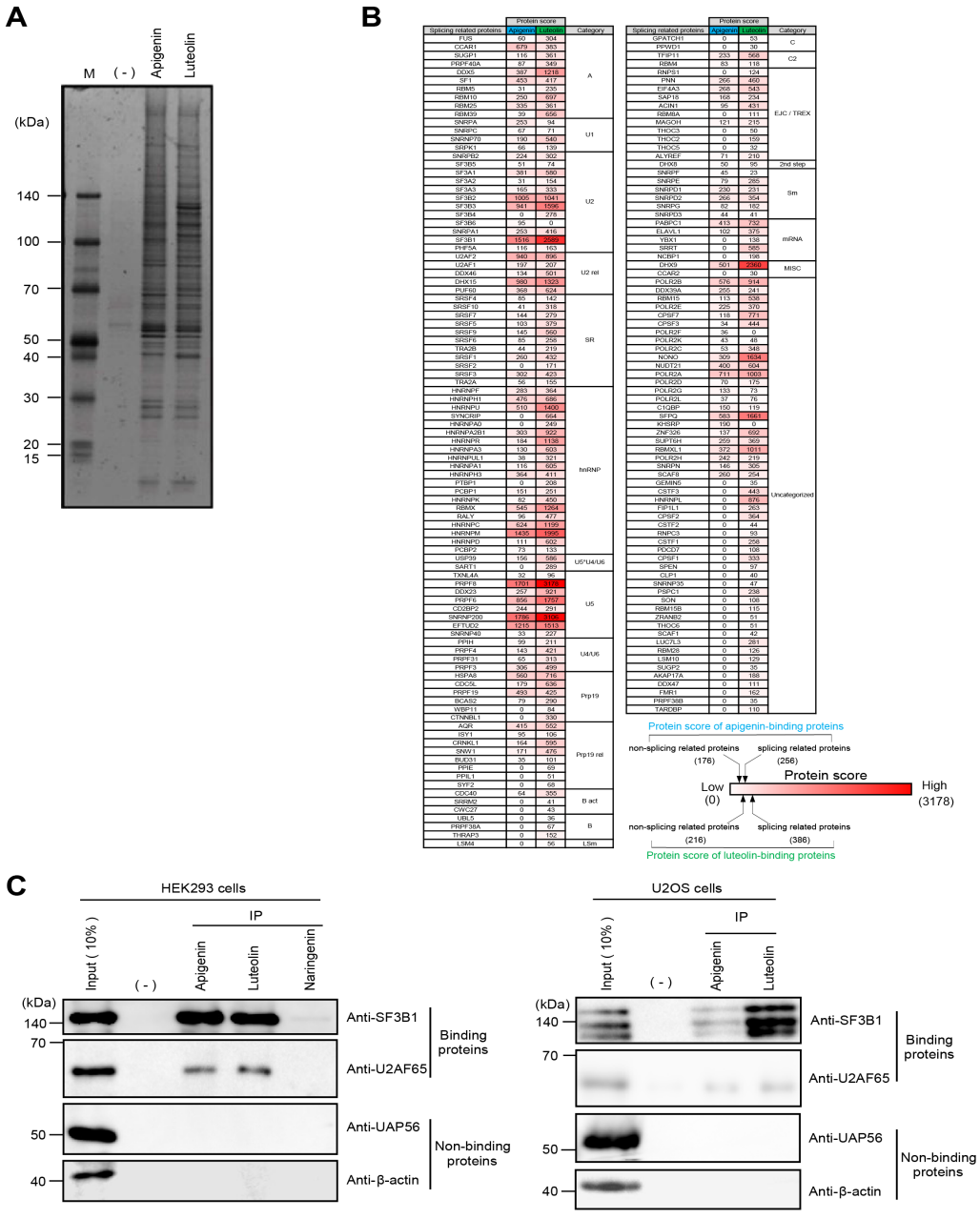

Figure S3. Detection of apigenin- and luteolin-binding proteins. (Related to Figure 3)

(A) Apigenin- and luteolin-binding proteins were purified from the nuclear extracts of HEK293 cells with unfixed (−) or flavonoid-fixed FG beads and were analyzed by silver staining. The binding proteins were analyzed by LC-MS/MS. M: Protein size marker.

(B) Splicing-related proteins binding to apigenin or luteolin. Prot_scores of control and apigenin- and luteolin-target proteins in Tables S1 and S2 were calculated using Mascot software (Matrix Science). Protein score is obtained by subtracting the prot_score of the control from that of apigenin or luteolin. Splicing-related proteins with protein score > 0 were extracted. When multiple protein scores were calculated for one protein, the highest value is listed. In the lower right bar, higher color intensity indicates a higher protein score. “Low” represents the lowest value, and “High” represents the highest value among the protein scores of splicing-related proteins. The black arrow indicates the average value of each protein score.

(C) Apigenin- and luteolin-binding proteins in HEK293 cells (left) and U2OS cells (right) were analyzed by western blotting. Naringenin was used as a negative control. The antibodies are indicated on the right side of each panel.

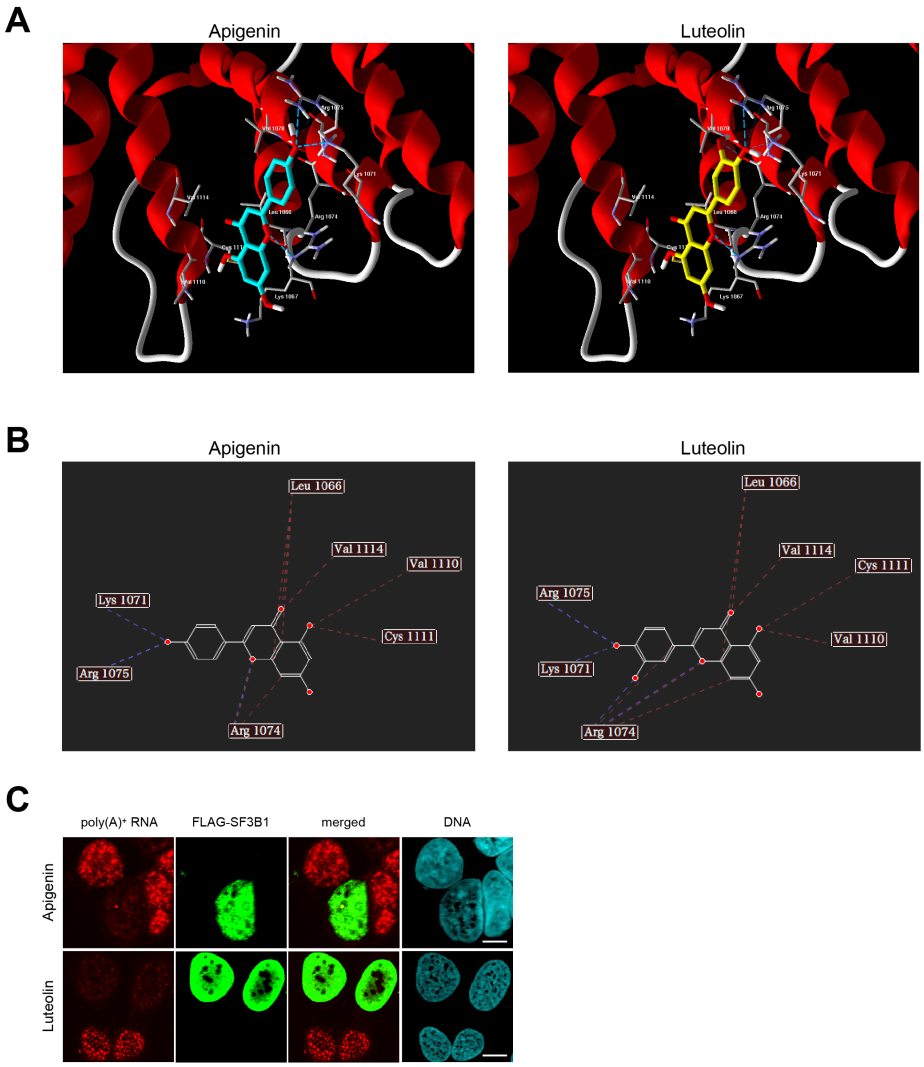

Figure S4. Binding of apigenin and luteolin in SF3B1. (Related to Figure 3)

(A) The crystal structure of human SF3B1 and E7107 was retrieved from the RCSB protein data bank (PDB code 5ZYA). The potential binding site of apigenin and luteolin in the SF3B complex was searched for and detected in the pocket near the branch point adenosine recognition site. The putative binding modes of apigenin and luteolin are displayed in sky blue and yellow, respectively.

(B) The simulation predicted that both apigenin and luteolin interact with several hydrophobic residues such as Leu1066, Val1114, Val1110, and Lys1067 of SF3B1. The Lys1071, Arg1074,

and Arg1075 are also the key residues for the hydrophobic interaction between E7107 and SF3B1, and are located near the BPA recognition site (Finci et al., 2018).

(C) The overexpression of FLAG-SF3B1 attenuated the flavonoid-induced nuclear poly(A)$^+$ RNA accumulation. Poly(A)$^+$ RNA (red), exogenously expressed FLAG-SF3B1 (green), and chromosomal DNA (blue) were visualized in U2OS cells. Scale bar, 10 μm.

Term	Count	P-Value
cellular nitrogen compound biosynthetic process	30/52	1.42E-05
RNA metabolic process	28/52	4.75E-05
cellular biosynthetic process	32/52	1.20E-04
transcription from RNA polymerase II promoter	16/52	1.39E-04
cellular nitrogen compound metabolic process	33/52	1.48E-04
organic substance biosynthetic process	32/52	1.75E-04
biosynthetic process	32/52	2.39E-04
organic cyclic compound biosynthetic process	26/52	2.96E-04
nucleic acid metabolic process	28/52	3.30E-04
nucleobase-containing compound metabolic process	30/52	3.51E-04

Term	Count	P-Value
intracellular transport	17/52	1.81E-06
RNA processing	13/52	3.26E-06
establishment of localization in cell	18/52	7.71E-06
mRNA metabolic process	11/52	8.83E-06
cellular localization	19/52	4.57E-05
macromolecule localization	19/52	1.81E-04
cellular macromolecule localization	14/52	2.18E-04
translation	9/52	2.66E-04
organic substance transport	18/52	2.96E-04
peptide biosynthetic process	9/52	3.48E-04

Term	Count	P-Value
cellular macromolecule metabolic process	48/75	5.50E-05
macromolecule metabolic process	50/75	9.81E-05
positive regulation of cellular metabolic process	24/75	1.45E-04
positive regulation of metabolic process	25/75	1.55E-04
positive regulation of macromolecule metabolic process	24/75	1.59E-04
regulation of molecular function	24/75	1.65E-04
regulation of protein metabolic process	22/75	2.07E-04
organic substance metabolic process	54/75	3.10E-04
positive regulation of protein metabolic process	16/75	3.62E-04
cellular metabolic process	52/75	4.85E-04

Term	Count	P-Value
organelle organization	361/1199	3.27E-20
cellular nitrogen compound metabolic process	549/1199	5.00E-20
cellular macromolecule metabolic process	662/1199	1.58E-18
nitrogen compound metabolic process	570/1199	3.70E-18
RNA processing	126/1199	1.75E-17
cellular component organization or biogenesis	522/1199	2.66E-17
nucleobase-containing compound metabolic process	486/1199	9.03E-16
heterocycle metabolic process	494/1199	9.60E-16
cellular component organization	504/1199	3.80E-15
cellular metabolic process	758/1199	4.02E-15

Figure S5. Gene ontology analysis of apigenin- and luteolin-induced A3SS, A5SS, MXE, and SE. (Related to Figure 4)

Common target genes of apigenin and luteolin (the number shown in bold) were uploaded to the DAVID database for GO analysis. Apigenin- and luteolin-target genes in U2OS cells were enriched for several GO terms categorized into “Biological Process.” Ten GO terms are listed in order of their p values. The denominator of the “Count” column indicates the number of genes assigned a DAVID ID among the uploaded target genes of apigenin and luteolin in each alternative splicing event. The numerator indicates the number of genes involved in each GO term.

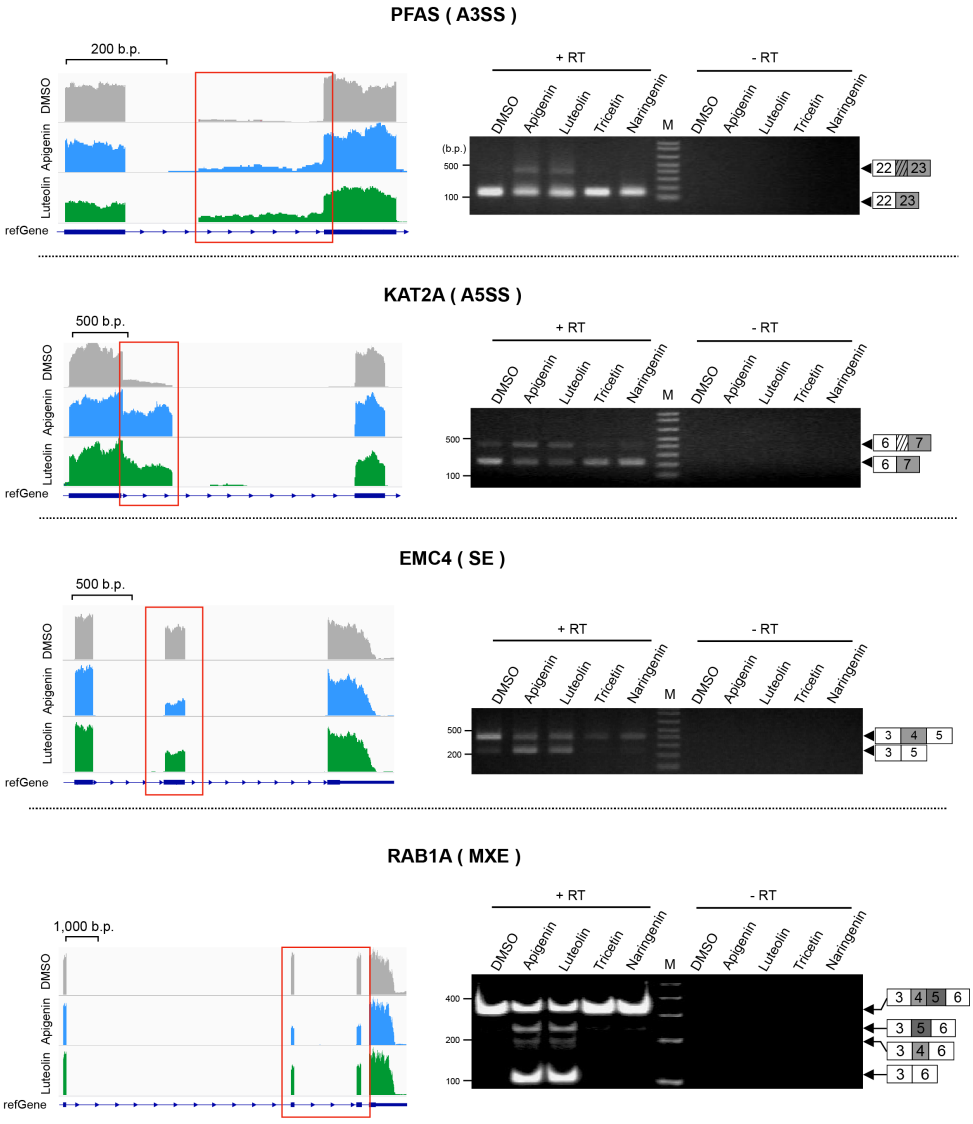

Figure S6. Validation of A3SS, A5SS, SE, and MXE regulated by apigenin and luteolin. (Related to Figure 4)

In the left panels, IGV snapshots of A3SS, A5SS, SE, and MXE induced by apigenin (blue) and luteolin (green) are shown. Gene structure is depicted at the bottom of each snapshot with horizontal lines indicating introns and boxes indicating exons. Red square lines surrounding alternative exons indicate regions affected by apigenin and luteolin. As shown in the right panels, RT-PCR was performed using total RNA samples in order to detect the apigenin- or luteolin-induced alternative splicing change. Representative results of triplicate experiments are shown. DNA size in base pairs (b.p.) is indicated on the left side. RT: reverse transcription. M: DNA size marker.

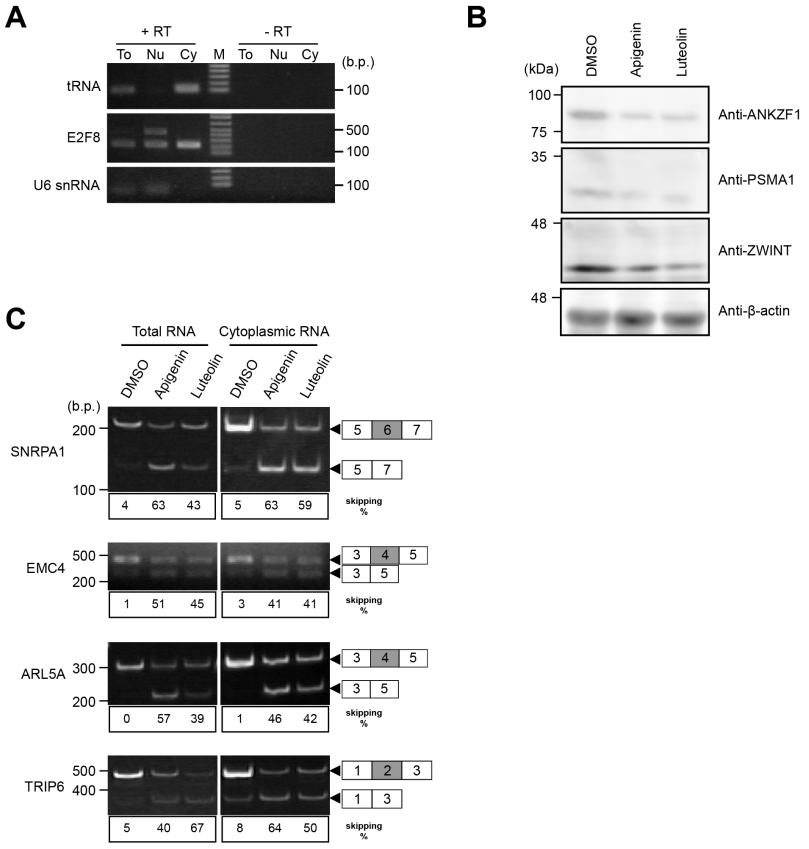

Figure S7. Expression of mRNA with altered splicing pattern in the cytoplasm. (Related to Figure 5)

(A) Fractionation of the nuclear, cytoplasmic, and total RNA was carried out. tRNA was detected as a dominant RNA species in the cytoplasmic fraction. *E2F8* mRNA was used to confirm that the fractionation had been successfully performed. U6 snRNA served as a nuclear marker. DNA size in base pairs (b.p.) is indicated on the right side. To: total RNA, Nu: nuclear RNA, Cy: cytoplasmic RNA. M: DNA size marker. RT: reverse transcription.

(B) Effect of flavonoids on protein expression. The U2OS cells were treated with apigenin or luteolin (75μM) for 24 h. Total cell extracts were subjected to SDS-PAGE and analyzed by Western blotting. Representative blots are shown. The antibodies are indicated on the right side of each panel.

(C) Skipped exon induced by apigenin and luteolin treatment was detected using total RNA and cytoplasmic RNA by RT-PCR. The digit panels below the photo show the percentage of exon skipping band intensity and representative results of triplicate experiments.

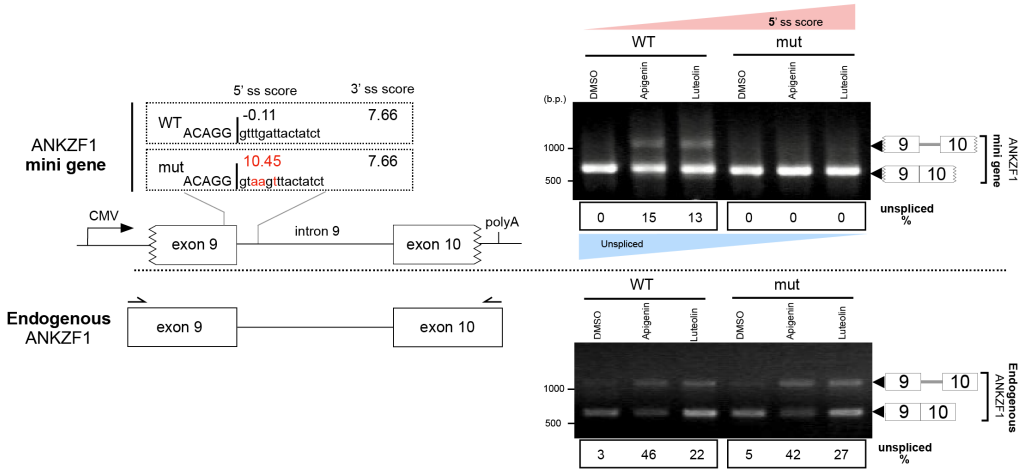

Figure S8. Apigenin and luteolin induce intron retention with weak splice sites. (Related to Figure 6)

The upper left panel presents a schematic representation of mini gene constructs affected by apigenin and luteolin. The CMV promoter and BGH poly(A) sites are shown. Jagged line in the figure of the exon indicates that the edges of the exons have been partially deleted in order to distinguish endogenous mRNA from transgene-derived mRNAs. The mutated nucleotides in each mutated-mini gene construct are shown in red, and the exon sequence is shown in upper case. The splice site (ss) score was calculated using MaxEntScan. The lower left panel presents a schematic representation of the endogenous gene. The locations of the primer that amplify the endogenous target are marked on the schematic representation of the endogenous gene (black arrows). Right panels show the results of RT-PCR. DNA size in base pairs (b.p.) is indicated on the left side. The mRNAs derived from the transgene are shown in the upper right panels, and endogenous mRNAs are shown in the lower right panels. The digit panels below the photo show the percentage of unspliced mRNA band intensity and representative results of triplicate experiments.

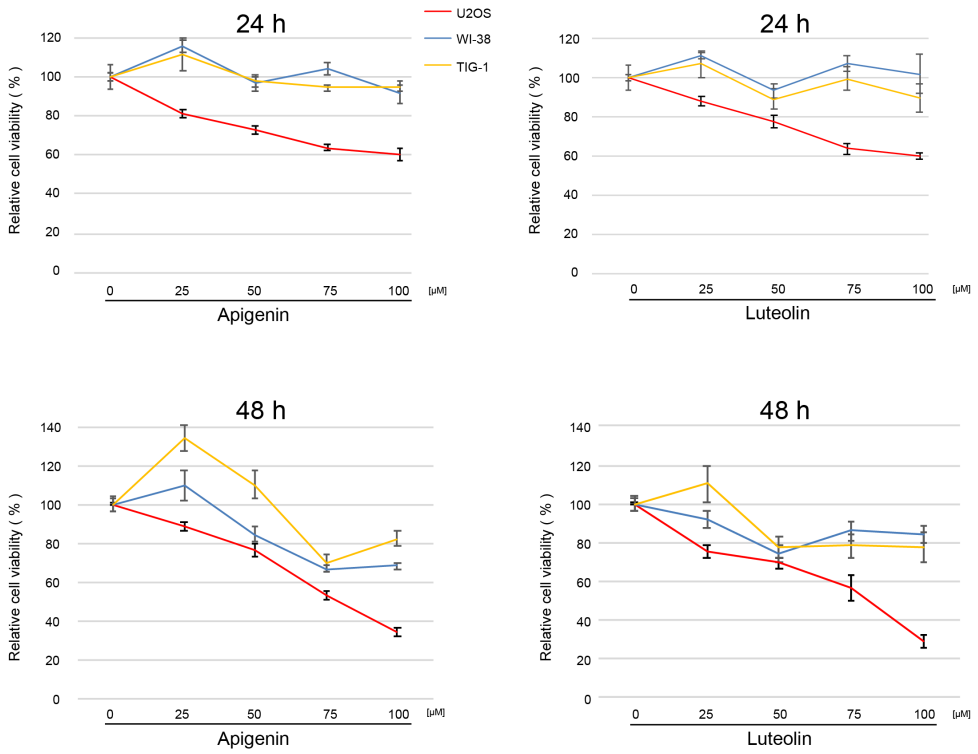

Figure S9. Inhibition of the proliferation in non-tumorigenic cells by apigenin and luteolin. (Related to Figure 8)

The proliferation of non-tumorigenic cells, WI-38 and TIG-1, treated with the indicated concentrations of each compound for 24 or 48 h and compared with that of U2OS cells. Cell viability was determined by MTT assay. Cell viability in comparison with that of DMSO-treated cells, set to 100%, is reported as mean ± SD of six independent experiments.

Table S4. The sequence of siRNAs in this study. (Related to Figures 2 and 3)

Name	Nucleotide sequence	Source
EGFP	GGGCACAAGCUGGAGUACAACUACA	Invitrogen
TAP	GAACUGGUUCAAGAUUACAAUUCCU	Invitrogen

SF3B1 siRNA was predesigned by IDT. The catalog number is hs.Ri.SF3B1.13.1.

TRANSPARENT METHODS

Cell culture

U2OS, HeLa, MCF7, HaCaT, and HEK293 cells were maintained in Dulbecco's Modified Eagle Medium (Wako, Kyoto, Japan) supplemented with 10% heat-inactivated fetal bovine serum at 37°C. WI-38 and TIG-1 cells were maintained in Eagle's minimum essential medium (Wako) supplemented with 10% heat-inactivated fetal bovine serum at 37°C.

Antibodies

The commercial antibodies used were as follows: anti-SF3B1 mouse monoclonal antibody (1:1000 dilution) (a kind gift from Robin Reed, Ph.D.), anti-U2AF65 mouse monoclonal antibody (1:1000 dilution) (also from Robin Reed, Ph.D.), anti-β-actin mouse monoclonal antibody (1:2000 dilution) (Sigma-Aldrich, St. Louis, MO), anti-SC35 mouse monoclonal antibody (1:2000 dilution) (Sigma-Aldrich), anti-FLAG M2 monoclonal antibody (1:1000 dilution) (Sigma-Aldrich), anti-ANKZF1 (1:500 dilution) (GeneTex, Irvine, CA), anti-PSMA1 (1:2000 dilution) (GeneTex), and anti-ZWINT (1:2000 dilution) (GeneTex). Anti-UAP56 rat polyclonal antibody, as described previously, was also used (Yamazaki et al., 2010).

Fluorescence in situ hybridization (RNA-FISH)

Cells (5×10^4 cells/mL) on coverslips in a 12-well plate were cultured for 24 h following inoculation, fixed with 10% formaldehyde in phosphate-buffered saline (PBS) for 20 min, and permeabilized in 0.1% Triton X-100 in PBS for 10 min. Cells were washed three times with PBS for 10 min to remove the detergent, once with 2× standard sodium citrate (SSC) for 5 min to exchange the buffer content, prehybridized with ULTRAhyb-Oligo Hybridization Buffer (Ambion, Austin, TX) for 1 h at 42°C in a humidified chamber, and then incubated overnight with 10 pmol Alexa Fluor 594-labeled oligo-dT_{45} probe (Molecular Probes, Eugene, OR) diluted with hybridization buffer. Cells were washed for 20 min each at 42°C with 2× SSC, 0.5× SSC, and 0.1× SSC. The nuclei were visualized with 4', 6-diamidino-2-phenylindole (DAPI). Fluorescent images were captured at random using a Zeiss Axioplan 2 (Carl Zeiss, Jena, Germany), equipped with an OLYMPUS DP70 camera (OLYMPUS, Tokyo, Japan). Confocal images were obtained by a FLUOVIEW FV10i microscope (OLYMPUS). The ratio of nuclear to total poly(A)$^+$ RNA signals was calculated using ImageJ software

(https://imagej.nih.gov/ij/) (version 1.51w), in accordance with the instructions.

Immunofluorescence

After RNA-FISH, the cells were washed once with PBS and then blocked with 6% bovine serum albumin (BSA) in PBS for 1 h at room temperature. The coverslips were incubated with the primary antibody in PBS containing 2% BSA, followed by secondary antibodies labeled with Alexa Fluor 488. Nuclei were visualized with DAPI.

Preparation of nuclear extracts

HEK293 or U2OS cells were centrifuged, washed twice with PBS, and very carefully suspended in double the pellet volume of hypotonic buffer [10 mM HEPES (pH 7.9), 1.5 mM $MgCl_2$, 10 mM KCl, 0.2 mM phenylmethylsulfonyl fluoride (PMSF), 0.5 mM dithiothreitol (DTT)]. The cells were kept on ice for 10 min, and the cell lysate was obtained by homogenization with a Dounce homogenizer (Wheaton, Millville, NJ). The cell lysate was collected by centrifugation at 13,000×g for 1 min. Half of the pellet volume of low-salt buffer [20 mM HEPES (pH 7.9), 1.5 mM $MgCl_2$, 20 mM KCl, 0.2 mM EDTA, 25% glycerol, 0.2 mM PMSF, 0.5 mM DTT] was then added to the pellet. After suspending the pellet, the same volume of high-salt buffer [20 mM HEPES (pH 7.9), 1.5 mM $MgCl_2$, 1.4 M KCl, 0.2 mM EDTA, 25% glycerol, 0.2 mM PMSF, 0.5 mM DTT] was added dropwise. The cell lysate was gently mixed by rotating at 4°C for 30 min and then centrifuged at 20,000×g for 15 min. The supernatant was collected and dialyzed for 3 h using dialysis buffer [20 mM HEPES (pH 7.9), 100 mM KCl, 0.2 mM EDTA, 20% glycerol, 0.2 mM PMSF, 0.5 mM DTT].

Construction of flavonoid-conjugated beads

Flavonoid was fixed with magnetic FG beads with an epoxy linker (Tamagawa Seiki, Iida, Japan) in the following way. In brief, flavonoid (final concentrations of 10 mM apigenin and 2 mM luteolin) was mixed with 0.5 mg of epoxy beads in N,N-dimethylformamide (DMF) containing K_2CO_3, which included a tenfold molar excess of flavonoid at 37°C overnight, and washed twice with 50% DMF and once with deionized water. Then, the beads were washed three times with 50% methanol (MeOH). The beads were suspended in 50% MeOH and stored at 4°C.

Purification of flavonoid-binding proteins

Flavonoid-fixed or control (unfixed) beads were mixed with HEK293 or U2OS cells nuclear extracts at 4°C for 4 h. After magnetic separation by washing thoroughly with 100 mM KCl buffer [20 mM HEPES-NaOH (pH 7.9), 100 mM KCl, 1 mM $MgCl_2$, 0.2 mM $CaCl_2$, 0.2 mM EDTA, 10% glycerol, 0.1% Nonidet P-40 (NP-40), 1 mM DTT, and 0.2 mM PMSF], the beads were subjected to sodium dodecyl sulfate polyacrylamide gel electrophoresis (SDS-PAGE) analysis and silver staining. To identify the flavonoid-binding proteins, LC-MS/MS analysis was performed by Q Exactive Plus (Thermo Fisher Scientific, Waltham, MA). The outputs of the LC-MS/MS analysis were prot_matches and prot_score. Prot_matches are the numbers of peptides identified (Tables S1 and S2). Prot_score was calculated using Mascot software (Matrix Science, London, UK). Protein scores shown in Figure S3B, and Tables S1 and S2 were calculated by subtracting the prot_score of the control from that of apigenin or luteolin.

Silver staining

The protein samples were mixed with 4× SDS buffer [190 mM Tris-HCl (pH 6.8), 40% glycerol, 0.8% SDS, 0.2% bromophenol blue, and 40 mM DTT] and boiled for 2 min. Protein separation was performed using SuperSep™ Ace, 5%–20%, 17-well (Wako). Silver staining of SDS-PAGE gels was carried out with Silver Staining Kit Protein (GE Healthcare, Little Chalfont, UK), in accordance with the manufacturer's protocol. Pictures were captured using the image analyzer LAS-1000 (Fujifilm, Tokyo, Japan).

Western blotting

Total cell extracts were prepared using RIPA buffer [25 mM Tris-HCl (pH 7.5), 150 mM NaCl, 1% NP-40, 1% sodium deoxycholate, 0.1% SDS, 0.2 mM PMSF and 0.5 mM DTT]. The total cell extracts and nuclear extracts were separated by SDS-PAGE and then electrotransferred to FluoroTrans PVDF Transfer Membranes (Pall, Ann Arbor, MI) using a Bio-Rad Trans-Blot cell (Bio-Rad, Hercules, CA). The blotted PVDF membrane was blocked with 5% skim milk/PBS containing 0.1% Tween 20 for 1 h at room temperature and reacted with the primary antibody with rotation at 4°C overnight. Blots were washed three times with PBS containing 0.1% Tween 20 for 10 min each and then incubated with horseradish peroxidase (HRP)-conjugated secondary antibody with rotation

at room temperature for 2 h. The blotted membranes were washed with PBS containing 0.1% Tween 20 for 10 min three times each, reacted with chemiluminescence reagent (Millipore, Darmstadt, Germany), and detected with the image analyzer LAS 4000 mini (GE Healthcare).

Docking studies

Molecular docking of apigenin and luteolin against the human SF3B1 was carried out using Molegro Virtual Docker ver. 6.0.1 (CLC bio, Aarhus, Denmark). The ligand structures were drawn by Marvin Sketch 5.11.5. The crystal structure of human SF3B1 bound to E7107 was downloaded from RCSB Protein Data Bank (PDB code: 5ZYA) and imported into the docking program according to the software's instructions, by removing all ligands and accessory molecules. Potential ligand-binding sites of proteins were calculated using the Molegro cavity detection algorithm. All parameters were set to default.

Total and cytoplasmic RNA isolation

U2OS cells (20% confluence) treated with or without flavonoids were recovered by trypsinization. Total RNA was isolated by Sepasol-RNA I Super G (Nacalai Tesque, Kyoto, Japan), in accordance with the manufacturer's instructions.

For cytoplasmic RNA preparation, the cells recovered by trypsinization were treated with lysis buffer [20 mM Tris-HCl (pH 8.0), 200 mM NaCl, 1 mM $MgCl_2$, 1% NP-40] on ice for 5 min. The cytoplasmic fraction was isolated by brief spinning. RNA in the cytoplasmic fraction was isolated by Sepasol-RNA I Super G, in accordance with the manufacturer's instructions.

Reverse transcription-polymerase chain reaction (RT-PCR)

Complementary DNA (cDNA) was synthesized from the extracted RNA using ReverTraAce (Toyobo, Osaka, Japan) and random 9-mer primer, in accordance with the manufacturer's instructions. PCR was performed using KOD FX Neo (Toyobo). The PCR products were visualized by a FAS-IV gel imaging system (Nippon Genetics, Tokyo, Japan). Amplified products were confirmed by sequencing. Quantitative RT-PCR (RT-qPCR) was performed with TB Green Premix Ex Taq II (Takara, Otsu, Japan) and analyzed on a Thermal Cycler Dice Real-Time System II (Takara). Each cDNA sample was prepared in triplicate. TATA-binding protein (*TBP*) was used to normalize each

sample. The amount of each mRNA was evaluated by threshold cycle (Ct) values. The relative levels of each mRNA were evaluated by the values of 2^[Ct (*TBP*) − Ct (each mRNA)]. Primer sets used in this study are listed in Table S3.

Assay for mini gene reporter fused *β-globin* FISH probe tag

U2OS cells on coverslips in a 12-well plate (20% confluence) were transfected with mini gene reporter fused *β-globin* FISH probe tag using Lipofectamine 2000 (Thermo Fisher Scientific), in accordance with the manufacturer's protocol, and cultured for 6 h. Then, each compound was added, and cells were further cultured for 24 h. Cells were fixed with 10% formaldehyde in PBS for 20 min and permeabilized with 0.1% Triton X-100 in PBS for 10 min. Cells were washed three times with PBS for 10 min to remove the detergent, once with 1× SSC containing 50% formamide for 5 min to exchange the buffer content, and hybridized with a FISH probe labeled at the 5' end with Alexa Fluor 546 (5'-cttcatccacgttcaccttgccccacagggcagtaacggcagacttctcctcaggagtcaggtgcaccat-3') overnight at 37°C in a humidified chamber. Cells were washed twice for 15 min at 42°C with 1× SSC/50% formamide and then washed for 5 min at 42°C with 2× SSC. Cells were prehybridized with ULTRAhyb-Oligo Hybridization Buffer for 1 h at 42°C in a humidified chamber, and then incubated overnight with 10 pmol Alexa Fluor 594-labeled oligo-dT_{45} probe diluted with hybridization buffer. Cells were washed for 20 min each at 42°C with 2× SSC, 0.5× SSC, and 0.1× SSC. The nuclei were visualized with DAPI.

Mini gene splicing assay

The *β-globin* reporter was kindly provided by Michael Antoniou, Ph.D. (Antoniou et al., 1998) The *β-globin* gene was amplified using this reporter. The amplified product was digested with KpnI and HindIII and then cloned into the KpnI and HindIII sites of pcDNA5/FRT/TO vector (Invitrogen, Carlsbad, CA). The genomic fragment of the apigenin- and luteolin-target gene was amplified from human genome DNA by PCR using KOD FX Neo (Toyobo). The amplified product was digested with BamHI and XhoI, and then cloned into the BamHI and XhoI sites of pcDNA5/FRT/TO vector using the wild type as a template; mutations were introduced by two-step PCR, as illustrated in Figures 6B, 6C, and S6. These mini genes were confirmed by sequencing. U2OS cells (20% confluence) in a six-well plate were cultured for 24 h after inoculation, and then transfected with

mini gene using Lipofectamine 2000 (Thermo Fisher Scientific), in accordance with the manufacturer's protocol, and cultured for 6 h. Then, each compound was added, and cells were cultured for 24 h. cDNA was synthesized from total RNA using ReverTraAce (Toyobo) and random 9-mer primer, in accordance with the manufacturer's instructions. PCR was performed using pcDNA5/FRT/TO-specific primers. The amplified products were separated by 1.0% agarose gel or 8.0% polyacrylamide gel. Primer sets for this analysis are described in Table S3. The PCR products were visualized by a FAS-IV (Nippon Genetics). Band intensity was quantified by ImageJ, in accordance with the instructions.

MTT assay

Cell proliferation was assayed colorimetrically by 3-(4,5-di-methylthiazol-2-yl)-2,5-diphenyltetrazolium bromide, yellow tetrazole (MTT) (Sigma-Aldrich) assay. The cells were inoculated at 8×10^3 cells/mL in a 96-well plate and cultured for 24 h. The test samples were added to each cell culture well and incubated for 24, 48, or 72 h. After 5 μL of MTT reagent (5 mg/mL) had been added to each well, the cells were incubated for 4 h. The cell culture plate was centrifuged at 400×g for 5 min, after which the supernatant was removed. Then, the cells were solubilized with 10 mM NH_4Cl containing 10% SDS (pH 7.0). Cell proliferation was estimated by measuring the optical absorbance at 600 nm.

Preparation of RNA-seq library

U2OS cells were treated with DMSO, 75 μM apigenin, or 75 μM luteolin for 24 h and then harvested. Total RNA was extracted from them with Sepasol-RNA I Super G. RNA-seq library was prepared using Truseq Stranded mRNA Library Prep Kit (Illumina, San Diego, CA). RNA-seq was conducted with two biological replicates from each group using NextSeq High Output (Illumina).

RNA-seq and global splicing analysis

The obtained sequence reads were mapped to the human hg38 genome using STAR (version 2.5.2b) (Dobin et al., 2013). Alternative splicing analysis was performed by rMATS (version 3.2.5) (Shen et al., 2014). Nonsignificant splicing events were filtered out using the threshold of false discovery rate (FDR) < 0.05. Gene ontology (GO) analysis was performed using Database for

Annotation, Visualization and Integrated Discovery (DAVID: version 6.7) (Huang et al., 2009a, 2009b). Integrative Genomics Viewer (IGV: version 2.3) (http://software.broadinstitute.org/software/igv/home) was used for visualization of the mapping results. Events with an FDR less than 0.05 were defined as significant splicing events, and these events were analyzed by RT-PCR, RT-qPCR, and bioinformatic analysis. Splice site score was calculated using MaxEntScan (Yeo and Burge, 2004). BPS score was calculated using the SVM-BP program (Corvelo et al., 2010).

siRNA or plasmid transfection

Transfection of siRNA or pcDNA3.1-FLAG-SF3B1 (Item # 82576, obtained from Addgene, Watertown, MA) was performed using Lipofectamine 2000 (Thermo Fisher Scientific) according to the manufacturer's instructions. The knockdown was performed for 48 h in SF3B1 and for 40 h in TAP. EGFP siRNA was used as a control. The sequence of siRNAs used in this study is listed in Table S4.

SUPPLEMENTAL REFERENCES

Antoniou, M., Geraghty, F., Hurst, J., and Grosveld, F. (1998). Efficient 3'-end formation of human β-globin mRNA in vivo requires sequences within the last intron but occurs independently of the splicing reaction. Nucleic Acids Res. *26*, 721–729.

Corvelo, A., Hallegger, M., Smith, C.W.J., and Eyras, E. (2010). Genome-Wide Association between Branch Point Properties and Alternative Splicing. PLoS Comput Biol *6*, e1001016.

Dobin, A., Davis, C.A., Schlesinger, F., Drenkow, J., Zaleski, C., Jha, S., Batut, P., Chaisson, M., and Gingeras, T.R. (2013). STAR: Ultrafast universal RNA-seq aligner. Bioinformatics *29*, 15–21.

Finci, L.I., Zhang, X., Huang, X., Zhou, Q., Tsai, J., Teng, T., Agrawal, A., Chan, B., Irwin, S., Karr, C., et al. (2018). The cryo-EM structure of the SF3b spliceosome complex bound to a splicing modulator reveals a pre-mRNA substrate competitive mechanism of action. Genes Dev. *32*, 309–320.

Huang, D.W., Sherman, B.T., and Lempicki, R.A. (2009a). Bioinformatics enrichment tools: paths toward the comprehensive functional analysis of large gene lists. Nucleic Acids Res. *37*, 1–13.

Huang, D.W., Sherman, B.T., and Lempicki, R.A. (2009b). Systematic and integrative analysis of large gene lists using DAVID bioinformatics resources. Nat. Protoc. *4*, 44–57.

Shen, S., Park, J.W., Lu, Z., Lin, L., Henry, M.D., Wu, Y.N., Zhou, Q., and Xing, Y. (2014). rMATS: Robust and flexible detection of differential alternative splicing from replicate RNA-Seq data. Proc. Natl. Acad. Sci. U. S. A. *111*, E5593–E5601.

Yamazaki, T., Fujiwara, N., Yukinaga, H., Ebisuya, M., Shiki, T., Kurihara, T., Kioka, N., Kambe, T., Nagao, M., Nishida, E., et al. (2010). The Closely Related RNA helicases, UAP56 and URH49, Preferentially Form Distinct mRNA Export Machineries and Coordinately Regulate Mitotic Progression. Mol. Biol. Cell *21*, 2953–2965.

Yeo, G., and Burge, C.B. (2004). Maximum Entropy Modeling of Short Sequence Motifs with Applications to RNA Splicing Signals. J. Comput. Biol. *11*, 377–394.